iScience

CellPress
OPEN ACCESS

Article

STUB1-mediated ubiquitination regulates the stability of GLUD1 in lung adenocarcinoma

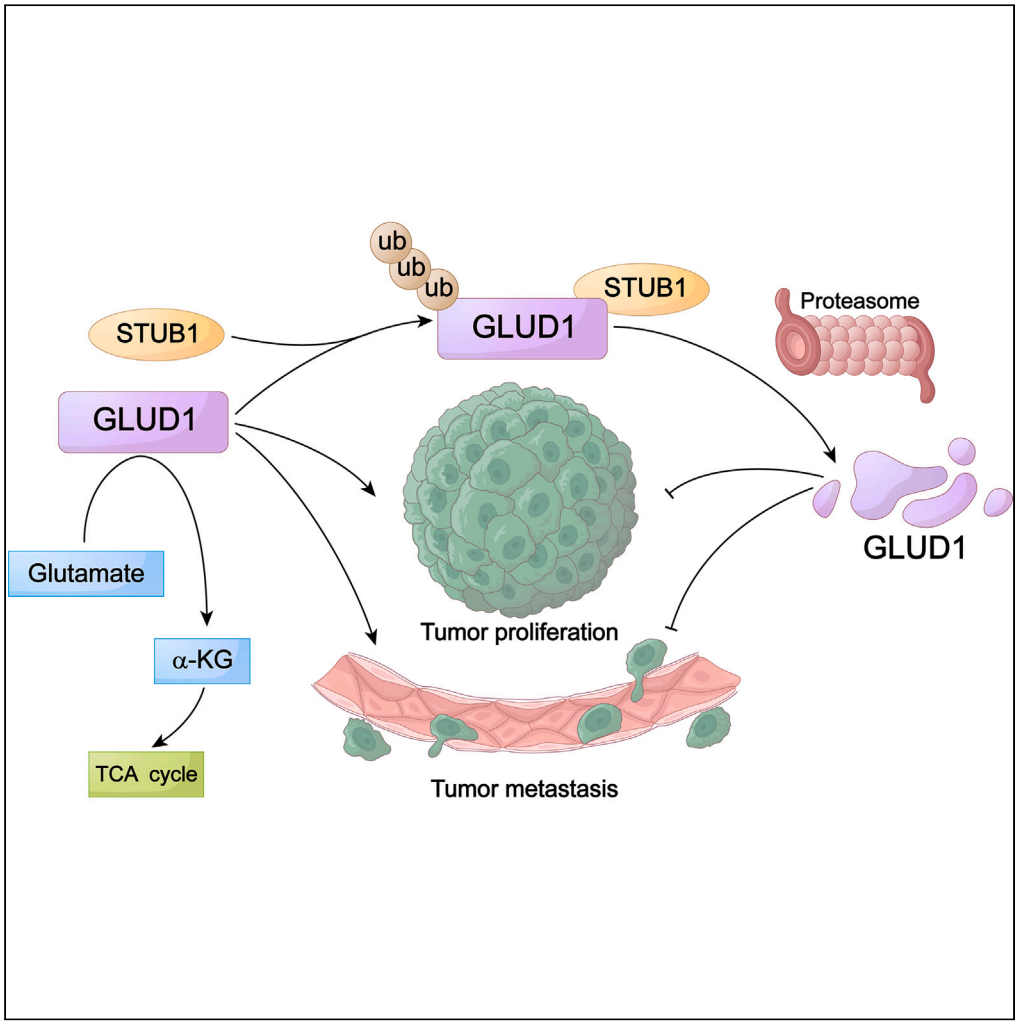

Qifan Hu, Jiapeng Lei, Zhujun Cheng, ..., Wenze Xun, Jian-Bin Wang, Tianyu Han

hantianyu87@163.com

Highlights

STUB1 ubiquitinates GLUD1 for proteasomal degradation in lung adenocarcinoma

STUB1 ubiquitinates GLUD1 on Lysine 503

Inhibiting the ubiquitination of GLUD1-K503 promotes tumorigenicity of LUAD cells

Hu et al., iScience 26, 107151
July 21, 2023
https://doi.org/10.1016/j.isci.2023.107151

iScience

CellPress
OPEN ACCESS

Article

STUB1-mediated ubiquitination regulates the stability of GLUD1 in lung adenocarcinoma

Qifan Hu,[1,2,3,10] Jiapeng Lei,[2,4,10] Zhujun Cheng,[5] Jing Xu,[2] Lei Wang,[2] Yi Yuan,[6] Mingxi Gan,[2] Yanan Wang,[1] Yilin Xie,[7] Lu Yao,[6] Keru Wang,[6] Yuhan Liu,[2] Wenze Xun,[2] Jian-Bin Wang,[2,3] and Tianyu Han[1,8,9,11,*]

SUMMARY

The dysregulation of glutamine metabolism provides survival advantages for tumors by supplementing tricarboxylic acid cycle. Glutamate dehydrogenase 1 (GLUD1) is one of the key enzymes in glutamine catabolism. Here, we found that enhanced protein stability was the key factor for the upregulation of GLUD1 in lung adenocarcinoma. We discovered that GLUD1 showed a high protein expression in lung adenocarcinoma cells or tissues. We elucidated that STIP1 homology and U-box-containing protein 1 (STUB1) was the key E3 ligase responsible for ubiquitin-mediated proteasomal degradation of GLUD1. We further showed that lysine 503 (K503) was the main ubiquitination site of GLUD1, inhibiting the ubiquitination at this site promoted the proliferation and tumor growth of lung adenocarcinoma cells. Taken together, this study clarifies the molecular mechanism of GLUD1 in maintaining protein homeostasis in lung adenocarcinoma, which provides a theoretical basis for the development of anti-cancer drugs targeting GLUD1.

INTRODUCTION

Metabolic reprogramming is one of the main characteristics of cancer cells, which provides substrates and energy for the survival and proliferation of cancer cells.[1,2] Enhanced glutamine metabolism is an important feature of cancer metabolic reprogramming, which provides survival advantages for cancer development by providing energy and macromolecular precursors required for biosynthesis.[3,4] Glutamate dehydrogenase (GLUD) is one of the key enzymes in glutamine catabolism. In the human body, GLUD has two subtypes, namely GLUD1 and GLUD2. Compared with GLUD2, GLUD1 has higher activity and less sensitivity to the activation of ADP.[5,6] GLUD1 converts glutamate to alpha-ketoglutarate (α-KG), an important intermediate of the tricarboxylic acid (TCA) cycle, thus providing a metabolic advantage to cancer cells.[7] It has been reported that GLUD1 plays an important role in TCA cycle, signal transduction, regulation of carbon and nitrogen metabolism, energy regulation, and maintenance of cell homeostasis.[8–12] GLUD1 is also reported to be closely associated with cancer progression. However, little is known about the regulation mechanism for GLUD1 in cancer progression, especially in its degradation mechanisms.

As a chaperone-dependent E3 ubiquitin ligase, STUB1 is expressed in most tissues,[13] especially in tissues with fast protein turnover and high metabolism. It contains three domains, the three tetrapeptide repeats at the N-terminal (TRP domain), the CC domain in the middle, and the U-box domain at the C-terminus. STUB1 can ubiquitinate target substrate proteins and thus regulate cellular physiological functions. For most substrate proteins, STUB1 mediates the ubiquitination-mediated degradation in the form of K48-linkage, while in a few cases, STUB1 can also mediate substrate ubiquitination in the form of K63- or K27-linkage. A variety of ubiquitin linking forms give substrate proteins different physiological functions.[14–16] STUB1 is also involved in the regulation of various signaling pathways, including NF-κB, Hippo, TGF-β, and other classical signaling pathways.[11,17–19] Researchers have found that STUB1 is associated with a variety of cancers, and has been proved to participate in the occurrence, proliferation, and invasion of a variety of malignant cancers through regulating a variety of carcinogenic proteins, including TLR, EGFR, HER2, and other receptor proteins significantly related to cancers.[20–22] But the molecular mechanisms for STUB1 in regulating the progression of lung cancer still need to be further clarified.

In this study, we found that GLUD1 knockdown significantly inhibited the proliferation and migration of lung cancer cells.[23] Further studies showed that GLUD1 was degraded mainly through the ubiquitin-proteasome

[1]Jiangxi Institute of Respiratory Disease, The First Affiliated Hospital of Nanchang University, Nanchang City, Jiangxi 330006, China

[2]School of Basic Medical Sciences, Nanchang University, Nanchang City, Jiangxi 330031, China

[3]Department of Thoracic Surgery, The First Affifiliated Hospital of Nanchang University, Nanchang City, Jiangxi 330006, China

[4]School of Basic Medical Sciences, Nanchang Medical College, Nanchang City, Jiangxi 330000, China

[5]Department of Burn, The First Affiliated Hospital of Nanchang University, Nanchang City, Jiangxi 330006, China

[6]School of Huankui Academy, Nanchang University, Nanchang City, Jiangxi 330031, China

[7]School of Queen Mary, Nanchang University, Nanchang City, Jiangxi 330031, China

[8]Jiangxi Clinical Research Center for Respiratory Diseases, Nanchang City, Jiangxi 330006, China

[9]China-Japan Friendship Jiangxi Hospital, National Regional Center for Respiratory Medicine, Nanchang City, Jiangxi 330200, China

[10]These authors contributed equally

[11]Lead contact

*Correspondence: hantianyu87@163.com

https://doi.org/10.1016/j.isci.2023.107151

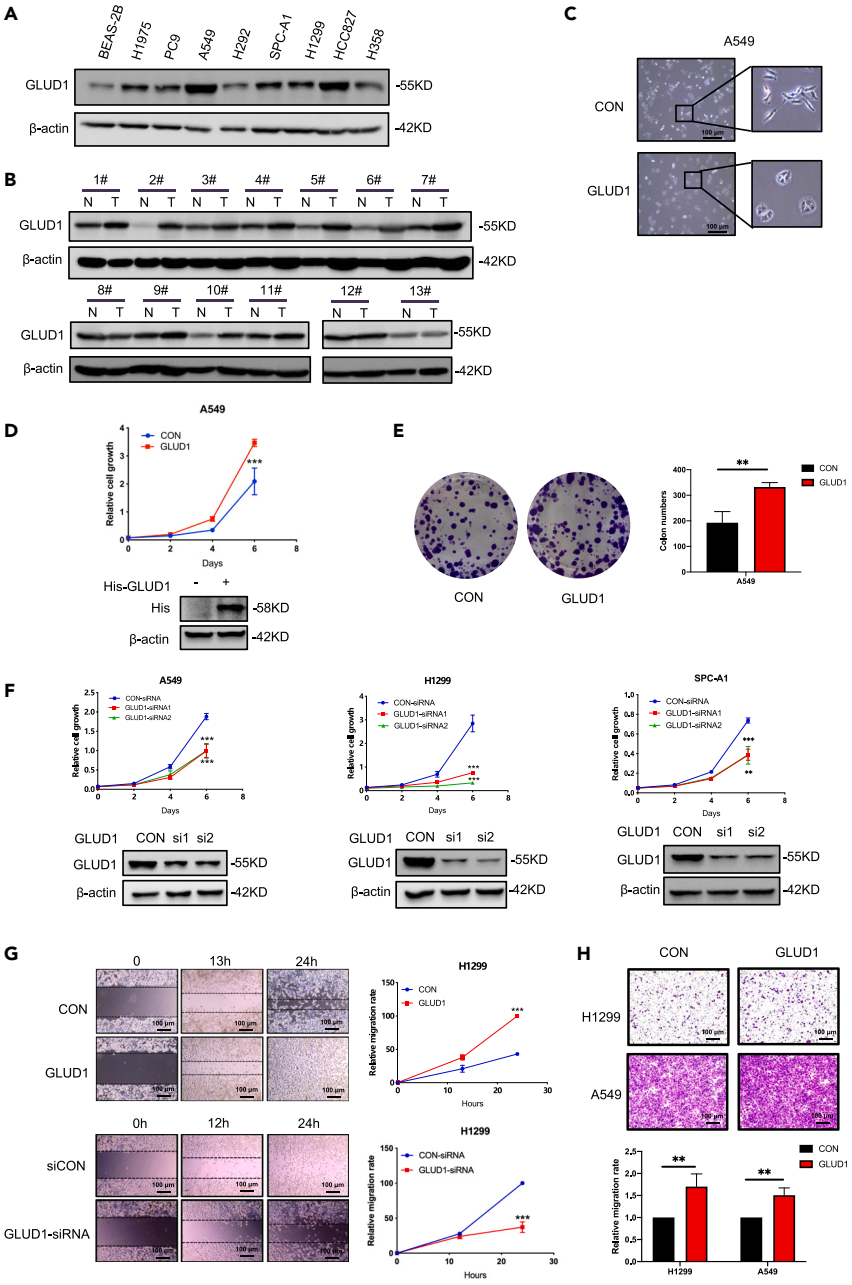

Figure 1. GLUD1 promotes the proliferation and migration of lung adenocarcinoma cells

(A) The protein levels of GLUD1 were detected in lung adenocarcinoma cell lines and normal bronchial epithelial cell BEAS-2B.

(B) The expression of GLUD1 protein in 13 lung adenocarcinoma tissues and paired adjacent normal tissues were detected by Western blot with anti-GLUD1 antibody.

(C) The wild-type A549 cells and A549 stable cell lines overexpressing His-GLUD1 were photographed using microscope.

(D) A549 cells were transfected with pcDNA3.1-His-GLUD1 plasmid or empty vector. Cell proliferation assay was performed (upper panel). Data represent the average of three independent experiments (mean ± SD). ***$p < 0.001$. The expression of His-GLUD1 was detected using Western blot (bottom panel).

(E) Colony formation assay. A549 cells were trypsinized, counted, and seeded in 6-well plates with 500 cells per well. After 10 days, cells were fixed and stained with crystal violet (left panel). Quantitative analysis of colony formation assay was performed using ImageJ software, the results represent the average of three independently repeated experiments (mean ± SD), **$p < 0.01$ (right panel).

Figure 1. *Continued*

(F) GLUD1 was knocked down by specific siRNA in A549 (left), H1299 (middle), and SPC-A1 (right) cell lines. Then, cell proliferation assay was performed. Data represent the average of three independent experiments (Mean ± SD). ***p < 0.001, **p < 0.01 (upper panel). The knockdown efficiencies of GLUD1 were detected by Western blot (bottom panel).

(G) H1299 cells were transfected with pcDNA3.1-His-GLUD1 plasmid (upper panel) or GLUD1 siRNAs (bottom panel). Cells were cultured in 1% FBS medium and wound healing assay was processed. At the indicated time, photographs were taken and the migration rate was calculated for statistical analysis (Mean ± SD). ***p < 0.001 (right panel).

(H) pcDNA3.1-His-GLUD1 plasmid was transfected into H1299 and A549 cells. Transwell chambers were used to inoculate H1299 cells (5×10^4 cells/well) and A549 cells (1×10^5 cells/well). After incubation for 10 h, the cells were fixed, stained, and photographed (upper panel). Cells migration was recorded at the indicated time for statistical analysis (Mean ± SD). **p < 0.01 (bottom panel).

pathway. We confirmed that STUB1, the E3 ubiquitin ligase, could interact with GLUD1 and promote the K48-linked ubiquitination, leading to the degradation of GLUD1. Furthermore, we confirmed that Lys503 was the key ubiquitination site of GLUD1 regulated by STUB1. Thus, our study clarified the role of GLUD1 in the proliferation and migration of lung adenocarcinoma and elucidated the molecular mechanism of STUB1 in regulating GLUD1 protein homeostasis, which provided a theoretical basis for the development of lung cancer therapeutic drugs by targeting GLUD1.

RESULTS

GLUD1 promotes the proliferation and migration of lung adenocarcinoma cells

To investigate the function of GLUD1 in lung adenocarcinoma cells, we first examined the expression of GLUD1 in lung adenocarcinoma cells and tissues. The protein expression of GLUD1 in all lung adenocarcinoma cells was significantly upregulated compared with human bronchial epithelial cell BEAS-2B (Figure 1A). Similar results were also obtained when we examined GLUD1 expression in lung adenocarcinoma tissues. Figure 1B showed that the expression of GLUD1 in 13 lung adenocarcinoma tissues was higher than that in adjacent normal tissues. We then used A549 cells to construct a stable cell line overexpressing GLUD1 to further explore its function in lung adenocarcinoma. We found that overexpression of GLUD1 affected the morphology of A549 cells, which are round and grow in clumps compared to wild-type A549 cells (Figure 1C), suggesting that GLUD1 might play an important role in lung adenocarcinoma cells. We next performed cell growth and colony formation assays to investigate the function of GLUD1. Overexpressing GLUD1 significantly promoted the proliferation of A549 cells (Figures 1D and 1E). However, the proliferation rates of lung adenocarcinoma cells were markedly attenuated when GLUD1 was knocked down by specific siRNAs (Figure 1F). We next detected the effects of GLUD1 expression on cell migration. Our wound healing assay showed that overexpression of GLUD1 significantly promoted the migration rate of H1299 cells, while knocking down GLUD1 markedly attenuated cell migration (Figure 1G). The transwell assay also showed that overexpression of GLUD1 promoted the migration of A549 and H1299 cells (Figure 1H). These data indicate that the proliferation and migration of lung adenocarcinoma cells depend on GLUD1 expression.

The overexpression of GLUD1 in lung adenocarcinoma is mainly regulated by the enhanced protein stability

To explore the regulation mechanisms of GLUD1 overexpression in lung adenocarcinoma, we first analyzed *GLUD1* TPM (transcripts per kilobase of exon model per million mapped reads) expression from gene expression profiling interactive analysis (GEPIA) platform and found that *GLUD1* TPM expression did not show a significant difference between tumor and normal tissues (Figures 2A and 2B). Next, we checked the mRNA levels of *GLUD1* in lung adenocarcinoma cell lines and BEAS-2B cells. The results showed that the mRNA levels of *GLUD1* in some lung adenocarcinoma cells were upregulated, and some were downregulated compared with BEAS-2B (Figure 2C). This indicated that the upregulation of GLUD1 protein in lung adenocarcinoma might not be due to the enhanced transcription of the *GLUD1* gene.

Protein homeostasis plays a crucial role during tumor progression. Thus, we examined the protein homeostasis of GLUD1 protein in lung adenocarcinoma cells. Firstly, we performed cycloheximide (CHX)-chase assays and measured the stability of GLUD1 protein in physiological conditions. The results showed that GLUD1 gradually decreased up to 24 h after treatment with CHX in BEAS-2B, A549, and H1299 cells. However, compared with A549 and H1299 cells, GLUD1 protein degradation was markedly accelerated under the same conditions in BEAS-2B cells (Figure 2D). We also found that the protein level of GLUD1 was

markedly decreased when A549 and H1299 cells were treated with CHX for 24 h, and this effect could be recovered via adding the proteasomal inhibitor MG132 or the lysosomal inhibitor chloroquine (CQ) (Figures 2E and 2F). The ubiquitination level of GLUD1 by adding MG132 or CQ was also examined and the result showed that the ubiquitination of GLUD1 was significantly increased by adding MG132, but not CQ, indicating the degradation by the ubiquitin-proteasomal pathway (Figure 2G). As GLUD1 is a mitochondrial enzyme and CQ treatment can also rescue the reduced protein expression induced by CHX treatment, we supposed that the stability of GLUD1 might also be regulated by mitophagy. Mdivi-1(Mitochondrial division inhibitor 1) is a mitophagy inhibitor and inhibits Dnm1 GTPase activity.[24] We then tested the GLUD1 protein expression by adding Mdivi-1 up to 24 h in A549 and H1299 cells. Figures 2H and 2I showed that Mdivi-1 treatment increased the GLUD1 protein expression in dosage dependent manner. However, Mdivi-1 could not affect *GLUD1* mRNA level as analyzed by RT-PCR (Figure 2J). These data suggest that GLUD1 can be degraded by both proteasomal degradation pathway and mitophagy pathway in lung adenocarcinoma.

E3 ligase STUB1 promotes the ubiquitination and degradation of GLUD1

To further investigate the mechanism of GLUD1 degradation by proteasome degradation pathway, we searched for potential E3 ligases of GLUD1 by E3 ligase analytical platform-UbiBrowserV2 and a series of E3 ligases were predicted (Figure 3A). Then, the protein level of GLUD1 was examined when overexpressing some potential E3 ligases in the database. Figure 3B showed that overexpressing STUB1 decreased GLUD1 protein expression in A549 cells, while overexpressing NEDD4L, UBE4A, UBE4B, SMURF1, MDM2, or SYVN1 did not affect GLUD1 protein expression (Figures S1A–S1F). Figure 3C showed that knockdown STUB1 increased GLUD1 protein expression. We also detected the expression pattern between GLUD1 and STUB1. Figure 3D showed that the protein expression of GLUD1 was negatively correlated with that of STUB1 in lung adenocarcinoma cells. In order to determine whether the STUB1 affects GLUD1 protein activity, we tested the activity of GLUD1 in A549 and H1299 cells and found that overexpression of STUB1 did not affect GLUD1 activity (Figures S2A and S2B). Next, we verified the interaction between GLUD1 and STUB1 through co-immunoprecipitation (co-IP). The results showed that GLUD1 and STUB1 interacted with each other (Figures 3E–3H). To test whether STUB1 regulates *GLUD1* at the transcriptional level, we examined *GLUD1* mRNA expression. Neither overexpression nor knockdown of STUB1 affected *GLUD1* mRNA expression (Figures 3I and 3J). The degradation rates of GLUD1 were then examined under STUB1 overexpression or knockdown conditions. The GLUD1 protein showed a significant decrease when A549 cells were treated with CHX for 12 h. The overexpression of STUB1 accelerated the degradation rate of GLUD1 to 12 h after the CHX treatment (Figure 3K). Instead, the GLUD1 protein degradation rate was slowed down in cells with STUB1 knockdown (Figure 3L). Next, we found that overexpressing STUB1 significantly increased the ubiquitination level of GLUD1 (Figure 3M). However, the ubiquitination level of GLUD1 was not affected by overexpressing the other E3 ligase predicted using UbiBrowser like NEDD4L, UBE4A, UBE4B, SMURF1, MDM2, or SYVN1 (Figures S3A–S3F). These data suggest that STUB1 is the key E3 ligase for GLUD1.

Next, we analyzed if STUB1 ubiquitinated GLUD1 through K48 or K63 linkages, both enabled substrates to degradation. We found that the K48-linked ubiquitination of GLUD1 increased significantly when overexpressing STUB1, and MG132 treatment could further enhance this type of ubiquitination of GLUD1 (Figure 3N). However, the K63-linked ubiquitination of GLUD1 was not affected by MG132 or CQ and there were no significant differences in the K63-linked ubiquitination when STUB1 was overexpressed (Figure 3O). Altogether, these data support the model that STUB1 ubiquitinates GLUD1 through K48-linkage, followed by degradation in the proteasomal pathway.

Lysine 503 of GLUD1 is the key ubiquitination site regulated by STUB1

We next want to identify the ubiquitination sites of GLUD1 regulated by STUB1. Using PhosphoSitePlus, we found that the K84, K183, K187, K191, K200, K363, K365, K386, K399, K480, and K503 were identified as the putative ubiquitination sites for GLUD1 (Figure 4A). Then, to investigate which sites were the major ubiquitination sites for STUB1, we constructed the GLUD1 plasmids containing indicated mutations (K84R, K183R, K187R, K191R, K200R, K363R, K365R, K386R, K399R, K480R, and K503R). We found that only the ubiquitination of the GLUD1^{K503R} mutant did not change when overexpressing STUB1 (Figure 4B). Whereas the ubiquitination of K84R, K183R, K187R, K191R, K200R, K363R, K365R, K386R, K399R, and K480R mutations still increased when overexpressing STUB1 (Figures 4C–4L).

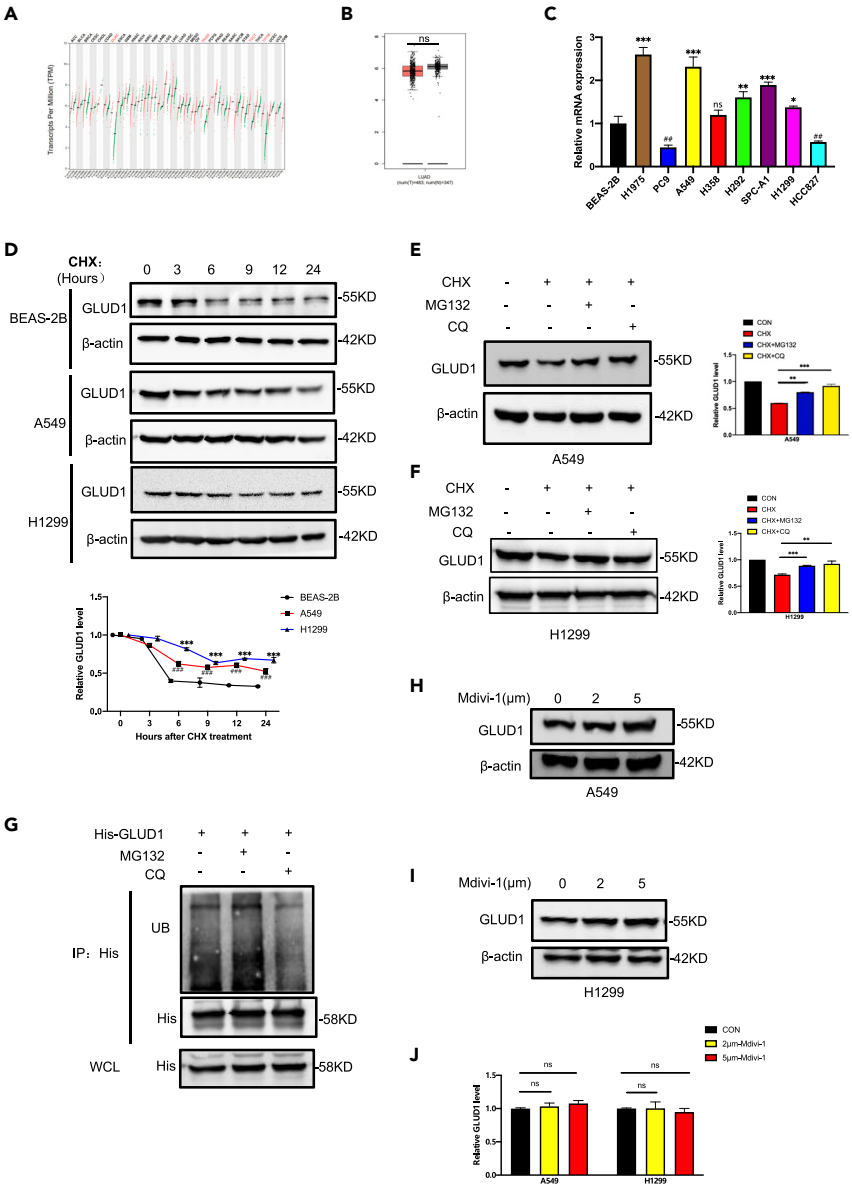

Figure 2. The overexpression of GLUD1 is mainly regulated by the enhanced protein stability in lung adenocarcinoma

(A and B) GEPIA (http://gepia.cancer-pku.cn) analysis for *GLUD1* TPM expression in tumor and normal tissues.

(C) The mRNA levels of *GLUD*1 were detected in lung adenocarcinoma cell lines and BEAS-2B. Relative GLUD1 expression over β-actin was quantified. Data represent the average of three independent experiments (mean ± SD). ns, $p > 0.05$; upregulation: ***$p < 0.001$, *$p < 0.05$; downregulation: ##$p < 0.01$.

(D) 20 μg/mL CHX was added to A549, H1299, and BEAS-2B cells, cells were collected at the indicated time. The degradation rate of GLUD1 was detected by Western blot (upper panel). Relative GLUD1 expression over β-actin was quantified (bottom panel). Data represent the average of three independent experiments (mean ± SD). H1299: ***$p < 0.001$; A549: ###$p < 0.001$.

(E and F) CHX (20 μg/mL) was added into A549 (E) and H1299 (F) cells for 24 h with or without MG132 (20 μM) or CQ (20 μM). GLUD1 protein was detected by Western blot (left panel). Relative GLUD1 expression over β-actin was quantified (right panel). Data represent the average of three independent experiments (mean ± SD). **$p < 0.01$ ***$p < 0.001$.

(G) A549 cells were transfected with pcDNA3.1-His-GLUD1 plasmid, and MG132 (20 μM) or CQ (20 μM) was added 12 h before sample collection. Co-IP was used to detect the ubiquitination level of GLUD1.

(H–J) Mdivi-1 at different concentrations was added into A549 and H1299 cells for 12 h, cells were collected and the mRNA and protein level of GLUD1 was detected by Western blot (H and I) and RT-PCR (J). Data represent the average of three independent experiments (mean ± SD). ns, $p > 0.05$.

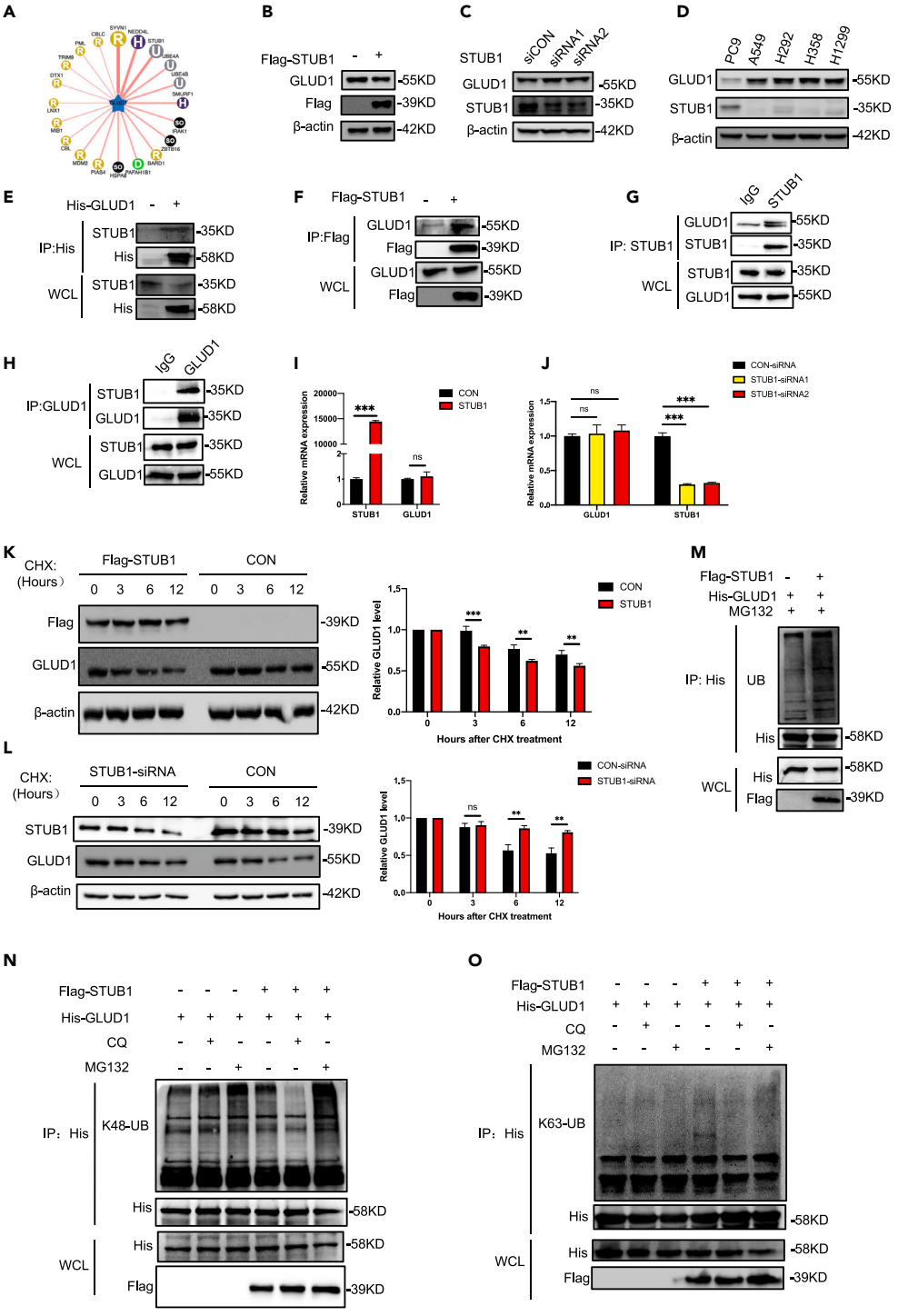

Figure 3. STUB1 interacts with GLUD1 and affects the stability of GLUD1 protein

(A) Ubibrowser was used to search for E3 ligases of GLUD1.

(B and C) In A549 cells, STUB1 was overexpressed (B) or knocked down (C) to detect GLUD1 protein by Western blot.

(D) The protein level of GLUD1 and STUB1 in PC9, A549, H292, H358, and H1299 cells were detected by Western blot.

(E and F) 293T cells were transfected with pcDNA3.1-His-GLUD1 plasmid (E) or pCMV-Flag-STUB1 (F). The immunoprecipitants were blotted with anti-His or anti-Flag antibodies. WCL: the whole cell lysate.

(G and H) In A549 cells, endogenous interaction between GLUD1 and STUB1 was tested using anti-STUB1 (G) and anti-GLUD1 (H) antibodies for co-IP, followed by Western blot detection.

Figure 3. *Continued*

(I and J) A549 cells were transfected with Flag-STUB1 plasmid (I) or STUB1 siRNAs (J), the mRNA expression of *GLUD1* was detected by RT-PCR. Data represent the average of three independent experiments (mean ± SD). ns, $p > 0.05$ ***$p < 0.001$.

(K and L) A549 cells were transfected with Flag-STUB1 (K) or STUB1 siRNAs (L), cells were treated with CHX (20 μg/mL) for 0, 3, 6, and 12 h. The protein stability of GLUD1 was detected by Western blot (left panel). Relative GLUD1 expression over β-actin was quantified (right panel). Data represent the average of three independent experiments (mean ± SD). ns, $p > 0.05$; **$p < 0.01$ ***$p < 0.001$.

(M) In A549 cells, Flag-STUB1 and His-GLUD1 plasmids were co-transfected and treated with MG132 for 12 h. The ubiquitination of GLUD1 was detected.

(N and O) In 293T cells, Flag-STUB1 and His-GLUD1 plasmids were co-transfected and treated with MG132 or CQ for 12 h. The K48-linkage ubiquitination (N) and K63-linkage ubiquitination (O) of GLUD1 was detected.

To further confirm whether K503 might be affected by other common modifications that usually occur on lysine, such as acetylation and succinylation, we tested the succinylation and acetylation levels of wild-type GLUD1 and GLUD1^{K503R} in A549 cells. We found that both acetylation and succinylation were not affected, indicating that K503 mainly underwent ubiquitination in lung adenocarcinoma cells (Figures S4A and S4B). We next measured the stability of GLUD1 and GLUD1^{K503R}. The GLUD1^{K503R} protein decreased lower than GLUD1 wild-type when cells were treated with CHX (Figure 4M). What is more, overexpression of STUB1 could not increase the degradation rate of GLUD1^{K503R} (Figure 4N). These data suggest that K503 of GLUD1 is the major ubiquitination site for STUB1.

The regulation of GLUD1 on cell viability relies on STUB1-mediated ubiquitination and degradation

To further examine whether the regulation of GLUD1 on cell viability was caused by the effect of STUB1 on its ubiquitination and degradation, we overexpressed GLUD1 and STUB1 in A549 and H1299 cells, and the cell growth assays revealed that STUB1 abated the enhanced proliferation mediated by GLUD1 overexpression (Figures 5A and 5B). In line with this, the transwell assay showed that overexpression of STUB1 could also reduce the migration ability of lung cancer cells overexpressing GLUD1 (Figures S5A and S5B). Then, we co-transfected GLUD1 plasmid and STUB1 siRNAs into lung cancer cells, the results showed that knocking down STUB1 further enhanced the tumor-promoting effects of GLUD1 overexpression (Figures 5C, 5D, S5C, and S5D).

We next established A549 cell lines stably overexpressing Flag-GLUD1 (GLUD1^{WT}) and lysine 503 mutant Flag-GLUD1 (GLUD1^{K503R}). Cell growth assay and colony formation assay showed that the proliferation rate of A549-GLUD1^{K503R} cells was more rapidly compared with A549-GLUD1^{WT} (Figures 5E and 5F). Meanwhile, the transwell migration assay showed that the migration rate of A549-GLUD1^{K503R} cells was markedly increased compared with A549-GLUD1^{WT} (Figure S5E). Furthermore, the xenograft assay was performed to determine the effect of GLUD1^{WT} and GLUD1^{K503R} mutant on tumor growth. Our data showed that A549 cells overexpressing GLUD1^{WT} showed an increase in tumor size and weight compared with wild-type A549 cells (Figure 5G), and A549-GLUD1^{K503R} further enhanced tumorigenicity compared with A549-GLUD1^{WT} cells (Figure 5H). To confirm these results, we performed immunohistochemistry (IHC) analysis of the tumor samples caused by wild-type A549, A549-GLUD1^{WT}, and A549-GLUD1^{K503R} using specificity antibodies recognizing Ki67 and TTF1. Ki67 is widely used as a proliferation marker in pathological assessments. TTF1 was demonstrated to be frequently suppressed in high-grade lung adenocarcinoma. We observed that the staining of Ki67 was markedly higher in the A549-GLUD1^{WT} group than that in the control group, while the Ki67 staining in the A549-GLUD1^{K503R} group was higher than that in the A549-GLUD1^{WT} group (Figure 5I). However, the staining of TTF1 was lower in the A549-GLUD1^{WT} group than that in the wild-type A549 group, and the A549-GLUD1^{K503R} group was lower compared with the A549-GLUD1^{WT} group (Figure 5J). Thus, our findings demonstrate that inhibiting the ubiquitination of GLUD1 on K503 enhances the proliferation and tumor growth of lung adenocarcinoma cells.

DISCUSSION

Glutamine metabolism has emerged as an important metabolic node in rapidly proliferating cancer cells. More and more studies have shown that glutamine metabolism plays an important role in tumor proliferation and metastasis.[25] Glutamine enters cancer cells through amino acid transporter and provides nitrogen and carbon sources for cancer cells. In addition, glutamine maintains the homeostasis of intracellular

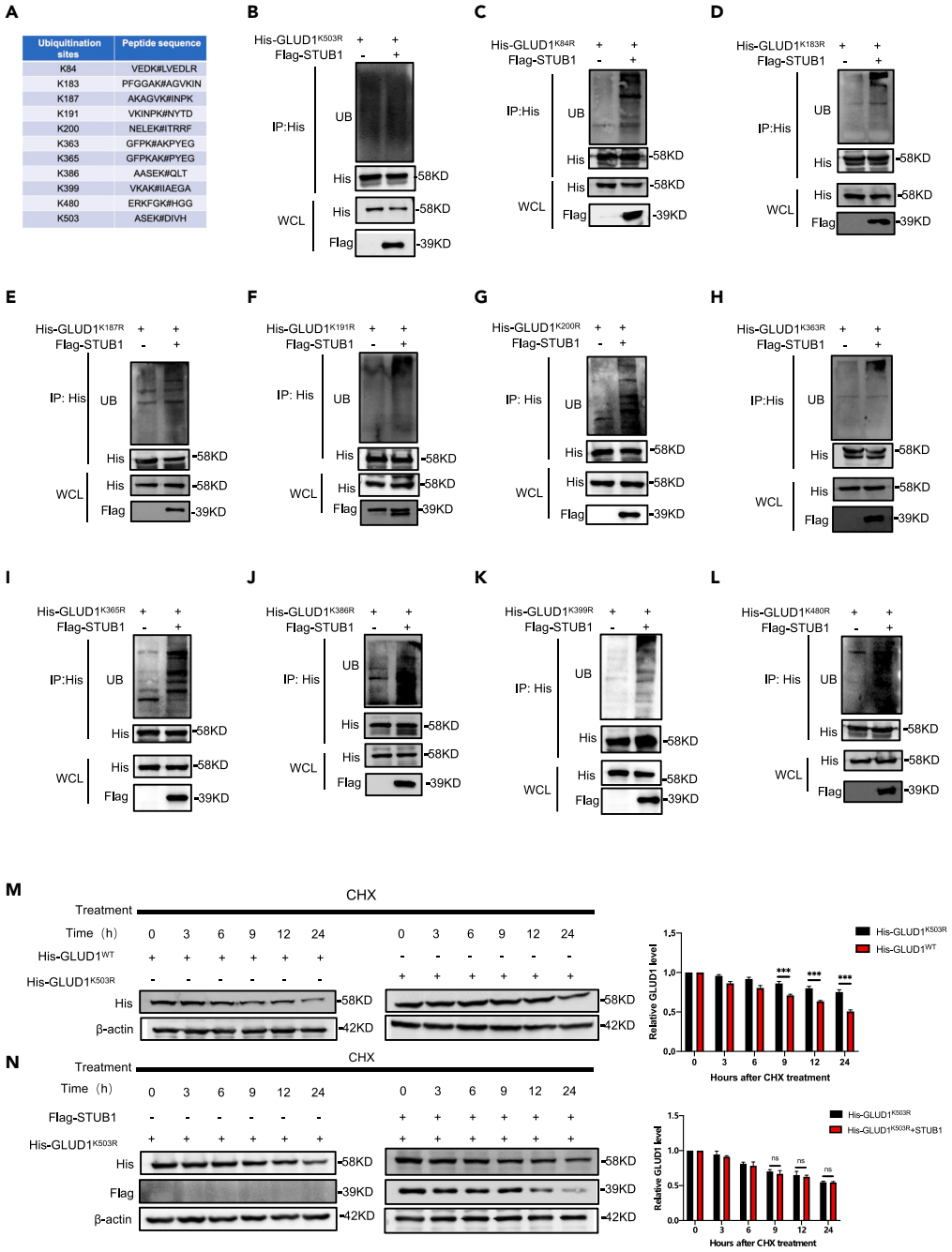

Figure 4. Lysine 503 of GLUD1 is the key ubiquitination site regulated by STUB1

(A) The ubiquitination sites of GLUD1 predicted by PhosphoSitePlus.

(B–M) The GLUD1 lysine residue mutation plasmids (lysine to arginine) are constructed based on the predicted ubiquitin sites of GLUD1. A549 cells were transfected with these plasmids and pCMV-Flag-STUB1, the ubiquitination levels of GLUD1 were detected. (B) GLUD1^{K503R} (C) GLUD1^{K84R} (D) GLUD1^{K183R} (E) GLUD1^{K187R} (F) GLUD1^{K191R} (G) GLUD1^{K200R} (H) GLUD1^{K363R} (I) GLUD1^{K365R} (J) GLUD1^{K386R} (K) GLUD1^{K399R} (L) GLUD1^{K480R} (M). In A549 cells, wild-type GLUD1 (His-GLUD1^{WT}) or His-GLUD1^{K503R} plasmids were overexpressed, CHX (20 μg/mL) was added to cells for 0, 3, 6, 9, 12, and 24 h, and the degradation rate of GLUD1 was detected by Western blot (left panel). Relative GLUD1 expression over β-actin was quantified. Data represent the average of three independent experiments (mean ± SD). ***$p < 0.001$ (right panel).

(N) A549 cells were transfected with His-GLUD1^{K503R} alone or co-transfected with Flag-STUB1, cells were treated with CHX (20 μg/mL) for 0, 3, 6, 9, 12, and 24 h. The degradation rate of GLUD1 was detected by Western blot (left panel). Relative GLUD1 expression over β-actin was quantified. Data represent the average of three independent experiments (mean ± SD). ns, $p > 0.05$ (right panel).

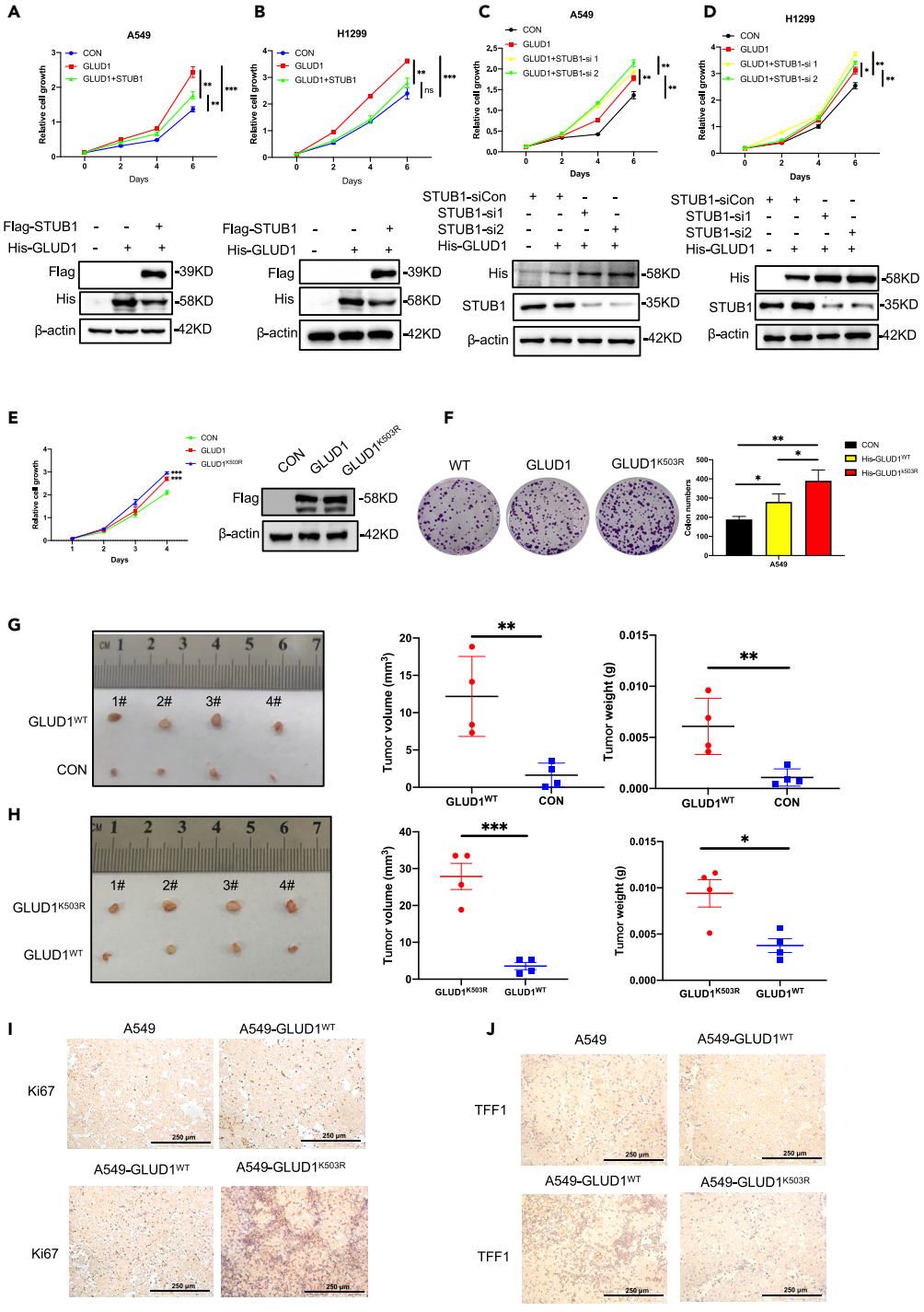

Figure 5. The regulation of GLUD1 on cell viability relies on STUB1-mediated ubiquitination and degradation

(A and B) A549 and H1299 cells were transfected with His-GLUD1 and Flag-STUB1 plasmid or control plasmid. Cell proliferation assays (upper panel) were performed. GLUD1 expression was detected by Western blot (bottom panel). Data represent the average of three independent experiments (mean ± SD). ns, $p > 0.05$, $^{**}p < 0.01$, $^{***}p < 0.001$.

(C and D) A549 and H1299 cells were transfected with His-GLUD1 and STUB1 siRNAs. Cell proliferation assay was performed (upper panel). GLUD1 expression was detected by Western blot (bottom panel). Data represent the average of three independent experiments (mean ± SD). $^{*}p < 0.05$, $^{**}p < 0.01$.

(E) Cell proliferation assay was performed in A549, A549-GLUD1, and A549-GLUD1^{K503R} cells (left panel). Protein expression was detected by Western blot (right panel). Data represent the average of three independent experiments (mean ± SD). $^{***}p < 0.001$.

Figure 5. *Continued*

(F) Colony formation assay were performed in A549, A549-GLUD1, and A549-GLUD1^{K503R} cells (left panel). The graph is statistical analysis (right panel). Data represent the average of three independent experiments (mean ± SD). *p < 0.05, **p < 0.01.

(G and H) A549-WT, A549-GLUD1, and A549-GLUD1^{K503R} cells were subcutaneously injected into the flanks of nude mice. After 25 days, tumors were dissected out and photographed (left panel). Tumor weight and volume were measured (right panel). The p value was calculated by paired t test. *p < 0.05, **p < 0.01.

(I and J) Immunohistochemical staining of tumors derived from nude mice using anti-Ki67 (I) or anti-TTF1 (J) antibodies. Magnification is ×200.

redox and participates in the regulation of glucose and lipid metabolism.[26–28] Many glutamine metabolic enzymes, such as GLS and GLUD1, have been reported as potential therapeutic targets in cancer therapy.

In this study, we observed that GLUD1 protein expression was upregulated in lung adenocarcinoma tissues compared with adjacent normal tissues. Overexpressing GLUD1 promoted the proliferation and migration of lung adenocarcinoma cells. These data suggested that GLUD1 had tumor-promoting functions in lung adenocarcinoma. In fact, researchers have found that GLUD1 could promote the proliferation of breast cancer and gastric cancer.[29,30] However, GLUD1 was also reported to be downregulated in some kinds of tumors, like liver cancer.[31] This suggested that GLUD1 might play different functions in different tumors. Until now, some studies have shown that GLUD1 played an important role in lung cancer. Researchers found that GLUD1 has a function in redox homeostasis in lung cancer cells by controlling the production of α-KG and subsequent metabolite fumarate. At the same time, the authors found R162 was a specific inhibitor of GLUD1.[32] In 2018, research reported that pleomorphic adenoma gene 1 (PLAG1) promoted GLUD1 upregulation, providing anti-anoikis and pro-metastatic signals in LKB1-deficient lung cancer. Mechanistically, the GLUD1 product α-KG activated CamKK2 for its binding to AMP-activated protein kinase (AMPK), which contributed to energy production that conferred anoikis resistance.[33]

The mechanism of GLUD1 degradation under physiological conditions has not been investigated. In this study, we elucidated the mechanism of post-translational modifications in the regulation of the protein levels of GLUD1 in lung adenocarcinoma cells. Mechanistically, the E3 ligase STUB1 degraded GLUD1 through the K48-linked ubiquitination in physiological conditions to promote its proteasomal degradation. We also elucidated that the K503 of GLUD1 was the key ubiquitination site for STUB1. As other post-translational modifications could also occur on lysine, we also detected two common modifications that occur on lysine, succinylation and acetylation. Both the acetylation and succinylation were not affected when mutating K503, indicating that K503 mainly underwent ubiquitination in lung adenocarcinoma cells. However, this still cannot rule out the other possible modifications on this site, such as lactylation, β-hydroxybutyrylation, etc., and the modification on this site may also vary depending on the type of cancer. In lung adenocarcinoma cells, we defined K503 as the key ubiquitination site for maintaining the stability of GLUD1, this provided an opportunity to develop drugs that target the GLUD1-K503 ubiquitination for lung adenocarcinoma treatment. It is reported that the E3 ligase RNF213 promoted GLUD1 ubiquitination and degradation under the condition of amino acid deprivation or mTORC1 inhibition in kidney renal clear cell carcinoma (KIRC) cells.[34] This result together with ours demonstrated that the regulation mechanism for GLUD1 protein degradation was variable according to different cancer types or survival environments. This also applied to the functional study of GLUD1 in cancer. As mentioned previously, GLUD1 played different roles in different cancers, indicating that it was necessary to consider the tumor type or different tumor subtypes within the same tumor when targeting GLUD1 for cancer treatment.

Mitophagy is an organelle-specific autophagy pathway that serves to maintain cell structure and function.[35] GLUD1 is mainly located in mitochondria, so we also attempted to explore whether GLUD1 could be degraded by the mitophagy pathway.[36] Adding the lysosomal inhibitor chloroquine (CQ) could recover the reduced expression of GLUD1 in cells treated with CHX for 24h. We further found that the mitophagy inhibitor Mdivi-1 could increase the GLUD1 protein expression in dosage dependent manner, indicating that mitophagy is another way for GLUD1 degradation. Thus, we discovered that GLUD1 could also be degraded by the mitophagy pathway. However, the mechanism of GLUD1 degradation through mitophagy needs to be further clarified.

The E3 ligase-STUB1 plays different roles in different cancers, either as an oncogene or tumor suppressor.[5] STUB1 affected the occurrence and development of tumors by degrading its substrate protein. In lung adenocarcinoma, scaffold protein PDLIM5 inhibited the interaction between STUB1 and transforming growth factor β effector protein SMAD3, thus protecting SMAD3 from degradation by STUB1-mediated

protein ubiquitination.[7] In addition, researchers showed that STUB1 preferentially targeted the mutated EGFR receptor and promoted its ubiquitination degradation under the treatment of vrinota (histone deacetylase inhibitor) in EGFR-C797S mutated lung adenocarcinoma, and finally inhibited the malignant development of EGFR-C797S mutated lung adenocarcinoma.[24] STUB1 was also reported to affect the degradation of metabolic enzymes. In ovarian cancer, STUB1 interacted with PKM2 and mediated its degradation through ubiquitination, thereby inhibiting aerobic glycolysis and tumor progression.[37] In breast cancer, STUB1 degraded PGK1 through ubiquitination and this effect could be further enhanced by lncRNA-LINC00926.[12] In our study, we identified that STUB1 regulated glutamine metabolism through ubiquitinating and degrading GLUD1, thus suppressing the progression of lung adenocarcinoma. These studies indicated that STUB1 was an important regulator in tumor metabolic reprogramming.

In conclusion, we found that STUB1 degraded GLUD1 through the K48-linked ubiquitination under physiological conditions and K503 residue of GLUD1 was the key ubiquitination site. GLUD1 could promote the proliferation and migration of lung adenocarcinoma cells and increase its tumorigenicity. These results indicate that GLUD1 is a potential therapeutic target for the treatment of lung adenocarcinoma.

Limitations of the study

In this study, we found that stably overexpressing GLUD1 affected the morphology of A549 cells, which were rounder and grow in clumps compared to wild-type A549 cells (Figure 1C). The data suggested that GLUD1 might have other important effects on lung adenocarcinoma cells. This needs to be further elucidated. In this study, we also found that GLUD1 could be degraded by mitophagy, and the molecular mechanism was unclear. We will study this in the future.

STAR★METHODS

Detailed methods are provided in the online version of this paper and include the following:

- KEY RESOURCES TABLE
- RESOURCE AVAILABILITY
  - Lead contact
  - Materials availability
  - Data and code availability
- EXPERIMENTAL MODEL AND STUDY PARTICIPANT DETAILS
  - Patient samples
  - Animal experiments *in vivo*
  - Cell culture
- METHOD DETAILS
  - Cell growth assay
  - Reverse transcription-polymerase chain reaction (RT-PCR)
  - Gene overexpression and knockdown
  - Transwell migration assay and scratch wound healing assay
  - Immunoprecipitation and Western blot
  - Measurement of GLUD1 activity
  - Stable cell lines construct
  - Immunohistochemistry
- QUANTIFICATION AND STATISTICAL ANALYSIS

SUPPLEMENTAL INFORMATION

Supplemental information can be found online at https://doi.org/10.1016/j.isci.2023.107151.

ACKNOWLEDGMENTS

This work were supported by the National Natural Science Foundation of China (82273258, 82030086, and 81902346), Natural Science Foundation of Jiangxi Province (20192ACB20024, 20212ACB216007, and 20212BAB216030), the Training Plan for Academic and Technical Leaders of Major Disciplines in Jiangxi Province (20204BCJ23023), Science and Technology Project of Jiangxi Provincial Health Commission (202130146), and Scientific Research Project of Cultivating Outstanding Young People in First Affiliated Hospital of Nanchang University (YQ202104).

AUTHOR CONTRIBUTIONS

T.H. and J.W. designed the study, and Q.H. put the design into practice. Q.H., J.L., Z.C., J.X., L.W., Y.Y., L.Y., K.W., W.X., and Y.X. designed and completed the experiments. Y.W., Y.L., and M.G. collected clinical tissues. T.H. and Q.H. analyzed the data and wrote the manuscript. J.W. and T.H. revised the paper. This manuscript was approved by all authors.

DECLARATION OF INTERESTS

The authors declare no competing interests.

Received: December 5, 2022
Revised: May 3, 2023
Accepted: June 12, 2023
Published: June 15, 2023

REFERENCES

1. Reznik, E., Luna, A., Aksoy, B.A., Liu, E.M., La, K., Ostrovnaya, I., Creighton, C.J., Hakimi, A.A., and Sander, C. (2018). A Landscape of Metabolic Variation across Tumor Types. Cell Syst. *6*, 301–313.e3. https://doi.org/10.1016/j.cels.2017.12.014.

2. Sun, L., Suo, C., Li, S.T., Zhang, H., and Gao, P. (2018). Metabolic reprogramming for cancer cells and their microenvironment: Beyond the Warburg Effect. Biochim. Biophys. Acta. Rev. Cancer *1870*, 51–66. https://doi.org/10.1016/j.bbcan.2018.06.005.

3. Hanahan, D., and Weinberg, R.A. (2011). Hallmarks of cancer: the next generation. Cell *144*, 646–674. https://doi.org/10.1016/j.cell.2011.02.013.

4. Pavlova, N.N., and Thompson, C.B. (2016). The Emerging Hallmarks of Cancer Metabolism. Cell Metab. *23*, 27–47. https://doi.org/10.1016/j.cmet.2015.12.006.

5. Paul, I., and Ghosh, M.K. (2015). A CHIPotle in physiology and disease. Int. J. Biochem. Cell Biol. *58*, 37–52. https://doi.org/10.1016/j.biocel.2014.10.027.

6. Liu, C.M., Yu, C.C., Lin, T., Liao, Y.W., Hsieh, P.L., Yu, C.H., and Lee, S.S. (2020). E3 ligase STUB1 attenuates stemness and tumorigenicity of oral carcinoma cells via transglutaminase 2 regulation. J. Formos. Med. Assoc. *119*, 1532–1538. https://doi.org/10.1016/j.jfma.2020.06.004.

7. Shi, Y., Wang, X., Xu, Z., He, Y., Guo, C., He, L., Huan, C., Cai, C., Huang, J., Zhang, J., et al. (2020). PDLIM5 inhibits STUB1-mediated degradation of SMAD3 and promotes the migration and invasion of lung cancer cells. J. Biol. Chem. *295*, 13798–13811. https://doi.org/10.1074/jbc.RA120.014976.

8. Luan, H., Mohapatra, B., Bielecki, T.A., Mushtaq, I., Mirza, S., Jennings, T.A., Clubb, R.J., An, W., Ahmed, D., El-Ansari, R., et al. (2018). Loss of the Nuclear Pool of Ubiquitin Ligase CHIP/STUB1 in Breast Cancer Unleashes the MZF1-Cathepsin Pro-oncogenic Program. Cancer Res. *78*, 2524–2535. https://doi.org/10.1158/0008-5472.CAN-16-2140.

9. Zhang, S., Guo, X., Liu, X., Zhong, Z., Yang, S., and Wang, H. (2021). Adaptor SH3BGRL promotes breast cancer metastasis through PFN1 degradation by translational STUB1 upregulation. Oncogene *40*, 5677–5690. https://doi.org/10.1038/s41388-021-01970-8.

10. Zhang, S., Guo, X., Liu, X., Zhong, Z., Yang, S., and Wang, H. (2022). Correction to: Adaptor SH3BGRL promotes breast cancer metastasis through PFN1 degradation by translational STUB1 upregulation. Oncogene *41*, 1227. https://doi.org/10.1038/s41388-021-02129-1.

11. Wei, C., Wu, J., Liu, W., Lu, J., Li, H., and Hai, B. (2021). Tripartite motif-containing protein 6 facilitates growth and migration of breast cancer through degradation of STUB1. Eur. J. Histochem. *65*, 3214. https://doi.org/10.4081/ejh.2021.3214.

12. Chu, Z., Huo, N., Zhu, X., Liu, H., Cong, R., Ma, L., Kang, X., Xue, C., Li, J., Li, Q., et al. (2021). FOXO3A-induced LINC00926 suppresses breast tumor growth and metastasis through inhibition of PGK1-mediated Warburg effect. Mol. Ther. *29*, 2737–2753. https://doi.org/10.1016/j.ymthe.2021.04.036.

13. Ballinger, C.A., Connell, P., Wu, Y., Hu, Z., Thompson, L.J., Yin, L.Y., and Patterson, C. (1999). Identification of CHIP, a novel tetratricopeptide repeat-containing protein that interacts with heat shock proteins and negatively regulates chaperone functions. Mol. Cell Biol. *19*, 4535–4545. https://doi.org/10.1128/MCB.19.6.4535.

14. Sane, S., Hafner, A., Srinivasan, R., Masood, D., Slunecka, J.L., Noldner, C.J., Hanson, A.D., Kruisselbrink, T., Wang, X., Wang, Y., et al. (2018). UBXN2A enhances CHIP-mediated proteasomal degradation of oncoprotein mortalin-2 in cancer cells. Mol. Oncol. *12*, 1753–1777. https://doi.org/10.1002/1878-0261.12372.

15. Choi, W.H., Yun, Y., Park, S., Jeon, J.H., Lee, J., Lee, J.H., Yang, S.A., Kim, N.K., Jung, C.H., Kwon, Y.T., et al. (2020). Aggresomal sequestration and STUB1-mediated ubiquitylation during mammalian proteaphagy of inhibited proteasomes. Proc. Natl. Acad. Sci. USA *117*, 19190–19200. https://doi.org/10.1073/pnas.1920327117.

16. Wang, S., Li, Y., Hu, Y.H., Song, R., Gao, Y., Liu, H.Y., Shu, H.B., and Liu, Y. (2013). STUB1 is essential for T-cell activation by ubiquitinating CARMA1. Eur. J. Immunol. *43*, 1034–1041. https://doi.org/10.1002/eji.201242554.

17. Wang, Y., Ren, F., Wang, Y., Feng, Y., Wang, D., Jia, B., Qiu, Y., Wang, S., Yu, J., Sung, J.J., et al. (2014). CHIP/Stub1 functions as a tumor suppressor and represses NF-kappaB-mediated signaling in colorectal cancer. Carcinogenesis *35*, 983–991. https://doi.org/10.1093/carcin/bgt393.

18. Shang, Y., Xu, X., Duan, X., Guo, J., Wang, Y., Ren, F., He, D., and Chang, Z. (2014). Hsp70 and Hsp90 oppositely regulate TGF-beta signaling through CHIP/Stub1. Biochem. Biophys. Res. Commun. *446*, 387–392. https://doi.org/10.1016/j.bbrc.2014.02.124.

19. Zhang, Y., Chen, Z., Luo, X., Wu, B., Li, B., and Wang, B. (2016). Cimetidine down-regulates stability of Foxp3 protein via Stub1 in Treg cells. Hum. Vaccin. Immunother. *12*, 2512–2518. https://doi.org/10.1080/21645515.2016.1191719.

20. Yang, M., Wang, C., Zhu, X., Tang, S., Shi, L., Cao, X., and Chen, T. (2011). E3 ubiquitin ligase CHIP facilitates Toll-like receptor signaling by recruiting and polyubiquitinating Src and atypical PKC{zeta. J. Exp. Med. *208*, 2099–2112. https://doi.org/10.1084/jem.20102667.

21. Hou, J., Deng, Q., Zhou, J., Zou, J., Zhang, Y., Tan, P., Zhang, W., and Cui, H. (2017). CSN6 controls the proliferation and metastasis of glioblastoma by CHIP-mediated degradation of EGFR. Oncogene *36*, 1134–1144. https://doi.org/10.1038/onc.2016.280.

22. Luan, H., Bailey, T.A., Clubb, R.J., Mohapatra, B.C., Bhat, A.M., Chakraborty, S., Islam, N., Mushtaq, I., Storck, M.D., Raja, S.M., et al. (2021). CHIP/STUB1 Ubiquitin Ligase Functions as a Negative Regulator of ErbB2 by Promoting Its Early Post-Biosynthesis Degradation. Cancers *13*, 3936. https://doi.org/10.3390/cancers13163936.

23. Coloff, J.L. (2018). Glutamate Dehydrogenase to the Rescue. Mol. Cell *69*,

1–2. https://doi.org/10.1016/j.molcel.2017.12.015.

24. Lin, C.Y., Huang, K.Y., Lin, Y.C., Yang, S.C., Chung, W.C., Chang, Y.L., Shih, J.Y., Ho, C.C., Lin, C.A., Shih, C.C., et al. (2021). Vorinostat combined with brigatinib overcomes acquired resistance in EGFR-C797S-mutated lung cancer. Cancer Lett. *508*, 76–91. https://doi.org/10.1016/j.canlet.2021.03.022.

25. Yang, L., Moss, T., Mangala, L.S., Marini, J., Zhao, H., Wahlig, S., Armaiz-Pena, G., Jiang, D., Achreja, A., Win, J., et al. (2014). Metabolic shifts toward glutamine regulate tumor growth, invasion and bioenergetics in ovarian cancer. Mol. Syst. Biol. *10*, 728. https://doi.org/10.1002/msb.20134892.

26. Porporato, P.E., Filigheddu, N., Pedro, J.M.B.S., Kroemer, G., and Galluzzi, L. (2018). Mitochondrial metabolism and cancer. Cell Res. *28*, 265–280. https://doi.org/10.1038/cr.2017.155.

27. Kouidhi, S., Ben Ayed, F., and Benammar Elgaaied, A. (2018). Targeting Tumor Metabolism: A New Challenge to Improve Immunotherapy. Front. Immunol. *9*, 353. https://doi.org/10.3389/fimmu.2018.00353.

28. Timmerman, L.A., Holton, T., Yuneva, M., Louie, R.J., Padró, M., Daemen, A., Hu, M., Chan, D.A., Ethier, S.P., van 't Veer, L.J., et al. (2013). Glutamine sensitivity analysis identifies the xCT antiporter as a common triple-negative breast tumor therapeutic target. Cancer Cell *24*, 450–465. https://doi.org/10.1016/j.ccr.2013.08.020.

29. Spinelli, J.B., Yoon, H., Ringel, A.E., Jeanfavre, S., Clish, C.B., and Haigis, M.C. (2017). Metabolic recycling of ammonia via glutamate dehydrogenase supports breast cancer biomass. Science *358*, 941–946. https://doi.org/10.1126/science.aam9305.

30. Wu, Y.J., Hu, Z.L., Hu, S.D., Li, Y.X., Xing, X.W., Yang, Y., and Du, X.H. (2019). Glutamate dehydrogenase inhibits tumor growth in gastric cancer through the Notch signaling pathway. Cancer Biomark. *26*, 303–312. https://doi.org/10.3233/CBM-190022.

31. Nwosu, Z.C., Battello, N., Rothley, M., Piorońska, W., Sitek, B., Ebert, M.P., Hofmann, U., Sleeman, J., Wölfl, S., Meyer, C., et al. (2018). Liver cancer cell lines distinctly mimic the metabolic gene expression pattern of the corresponding human tumours. J. Exp. Clin. Cancer Res. *37*, 211. https://doi.org/10.1186/s13046-018-0872-6.

32. Jin, L., Li, D., Alesi, G.N., Fan, J., Kang, H.B., Lu, Z., Boggon, T.J., Jin, P., Yi, H., Wright, E.R., et al. (2015). Glutamate dehydrogenase 1 signals through antioxidant glutathione peroxidase 1 to regulate redox homeostasis and tumor growth. Cancer Cell *27*, 257–270. https://doi.org/10.1016/j.ccell.2014.12.006.

33. Jin, L., Chun, J., Pan, C., Kumar, A., Zhang, G., Ha, Y., Li, D., Alesi, G.N., Kang, Y., Zhou, L., et al. (2018). The PLAG1-GDH1 Axis Promotes Anoikis Resistance and Tumor Metastasis through CamKK2-AMPK Signaling in LKB1-Deficient Lung Cancer. Mol. Cell *69*, 87–99.e7. https://doi.org/10.1016/j.molcel.2017.11.025.

34. Shao, J., Shi, T., Yu, H., Ding, Y., Li, L., Wang, X., and Wang, X. (2022). Cytosolic GDH1 degradation restricts protein synthesis to sustain tumor cell survival following amino acid deprivation. EMBO J. *41*, e110306. https://doi.org/10.15252/embj.2021110306.

35. Okamoto, K. (2014). Organellophagy: eliminating cellular building blocks via selective autophagy. J. Cell Biol. *205*, 435–445. https://doi.org/10.1083/jcb.201402054.

36. Mastorodemos, V., Kotzamani, D., Zaganas, I., Arianoglou, G., Latsoudis, H., and Plaitakis, A. (2009). Human GLUD1 and GLUD2 glutamate dehydrogenase localize to mitochondria and endoplasmic reticulum. Biochem. Cell. Biol. *87*, 505–516. https://doi.org/10.1139/o09-008.

37. Shang, Y., He, J., Wang, Y., Feng, Q., Zhang, Y., Guo, J., Li, J., Li, S., Wang, Y., Yan, G., et al. (2017). CHIP/Stub1 regulates the Warburg effect by promoting degradation of PKM2 in ovarian carcinoma. Oncogene *36*, 4191–4200. https://doi.org/10.1038/onc.2017.31.

STAR★METHODS

KEY RESOURCES TABLE

REAGENT or RESOURCE	SOURCE	IDENTIFIER
Antibodies		
GLUD1 Polyclonal antibody	Proteintech	Cat No:14299-1-AP
Ubiquitin Polyclonal antibody	Proteintech	Cat No:10201-2-AP
His-Tag Monoclonal antibody	Proteintech	Cat No:66005-1-Ig
DYKDDDDK tag Monoclonal antibody	Proteintech	Cat No:66008-4-Ig
Anti-STUB1 Recombinant Rabbit Monoclonal Antibody	HUABIO	Cat No: ET7108-65
Beta Actin Monoclonal antibody	Origene	Cat No: TA811000
K48-linkage Specific Polyubiquitin (D9D5) Rabbit mAb	Cell Signaling	Cat No:8081S
K63-linkage Specific Polyubiquitin (D7A11) Rabbit mAb	Cell Signaling	Cat No:5621
Anti-Ki67 antibody	abcam	Cat No: ab15580
Anti-TTF1 antibody (EP1584Y)	abcam	Cat No: ab76013
Anti-Succinyllysine Mouse mAb	PTM BIO	Cat No: PTM-419
Anti-Acetyllysine Rabbit mAb	PTM BIO	Cat No: PTM-105RM
Bacterial and virus strains		
TSINGKE TSC-C01Trelief-5a Chemically Competent	Tsingke Biological Technology	TSC-C01
Biological samples		
Human lung tumor and normal lung tissues	First Affiliated Hospital of Nanchang University	N/A
Chemicals, peptides, and recombinant proteins		
Chloroquine (CQ)	Sigma-Aldrich	C6628
Cycloheximide (NSC-185)	Selleck	S7418
MG132	Biovision	C1791
siTran 2.0 siRNA transfection reagent	OriGene	TT320002
SuperFectin DNA Transfection Reagent kit	Pufei	2102-100
Foetal Bovine Serum	SORFA	SX1500
TRTGene reagent	Genestar	P118-05
PrimeScript™ RT reagent Kit with gDNA Eraser	Takara	RR047A
SYBR Green Premix Ex Taq II kit	Takara	RR820A
Critical commercial assays		
Micro Glutamic Acid Dehydrogenase (GDH) Assay Kit	Solarbio	BC1465
Deposited data		
N/A		
Experimental models: Cell lines		
Human bronchial epitherial mesothelial cell lines: BEAS-2B	National Collection of Authenticated Cell Clutures	SCSP-5067
Human lung cancer cell line: HCC827	National Collection of Authenticated Cell Clutures	1101HUM-PUMC000478

(*Continued on next page*)

Continued

REAGENT or RESOURCE	SOURCE	IDENTIFIER
Human lung cancer cell line: NCI-H358	National Collection of Authenticated Cell Clutures	1101HUM-PUMC000470
Human lung cancer cell line: NCI-H1975	National Collection of Authenticated Cell Clutures	1101HUM-PUMC000252
Human lung cancer cell line: PC-9	National Collection of Authenticated Cell Clutures	4201PAT-CCTCC01380
Human lung cancer cell line: A549	National Collection of Authenticated Cell Clutures	1101HUM-PUMC000002
Human lung cancer cell line: NCI-H1299	National Collection of Authenticated Cell Clutures	1101HUM-PUMC000469
Human lung cancer cell line: NCI-H292	National Collection of Authenticated Cell Clutures	1101HUM-PUMC000233
Human lung cancer cell line: SPC-A1	BLUEFBIO	BFN60800698
Experimental models: Organisms/strains		
BALB/c nude mice	GemPharmatech Co., Ltd	D000521
Oligonucleotides		
Primers for RT-PCR, see Table S1	Tsingke Biological Technology	N/A
Primers for construct plasmids, see Table S1	Tsingke Biological Technology	N/A
Recombinant DNA		
pcDNA3.1-His-GLUD1 plasmid	This paper	N/A
pCDH-Flag-GLUD1 plasmid	This paper	N/A
pcDNA3.1-His - GLUD1-K84R plasmid	This paper	N/A
pcDNA3.1-His - GLUD1-K183R plasmid	This paper	N/A
pcDNA3.1-His GLUD1-K187R plasmid	This paper	N/A
pcDNA3.1-His - GLUD1-K191R plasmid	This paper	N/A
pcDNA3.1-His - GLUD1-K200R plasmid	This paper	N/A
pcDNA3.1-His - GLUD1-K363R plasmid	This paper	N/A
pcDNA3.1-His GLUD1-K365R plasmid	This paper	N/A
pcDNA3.1-His GLUD1-K386R plasmid	This paper	N/A
pcDNA3.1-His - GLUD1-K399R plasmid	This paper	N/A
pcDNA3.1-His - GLUD1-K480R plasmid	This paper	N/A
pcDNA3.1-His - GLUD1-K503R plasmid	This paper	N/A
pCMV-Flag-NEDD4L plasmid	This paper	N/A
pCMV-Flag-UBE4A plasmid	This paper	N/A
pCMV-Flag-UBE4B plasmid	This paper	N/A
pCMV-Flag-SMURF1 plasmid	This paper	N/A
pCMV-HA-SYVN1 plasmid	miaolingbio	P35682
Software and algorithms		
GraphPad Prism 8.0	GraphPad Prism Software	N/A
Image J	Schneider	N/A
Other		

RESOURCE AVAILABILITY

Lead contact

Further information and requests for resources and reagents should be directed to and will be fulfilled by the Lead Contact, Tianyu Han at hantianyu87@163.com.

Materials availability

This study did not generate new unique reagents.

Data and code availability

- Data: All the data reported in this study will be shared by the lead contact upon request.
- Code: This paper does not report original code.
- Additional information: Any additional information required to reanalyze the data reported in this paper is available from the lead contact upon request.

EXPERIMENTAL MODEL AND STUDY PARTICIPANT DETAILS

Patient samples

Lung adenocarcinoma and paired normal tissues samples were kindly provided by Dr. Bentong Yu in the Department of General Surgery from the First Affiliated Hospital of Nanchang University (Jiangxi Nanchang). All samples were collected with patients' informed consent and then frozen and preserved in -80°C. The detailed clinical information of all the patients including sex, age, race and clinical-pathological information is presented in Table S2. The subject was approved by the Medical Research Ethics Committee of First Affiliated Hospital of Nanchang University.

Animal experiments *in vivo*

4-week-old male BALB/c-Nude mice were purchased from Gempharmatech Co., Ltd (Jiangsu, China). All mice were lived in the SPF animal facility of the Institute of Translational Medicine at Nanchang University and experimental procedures were approved by the Institutional Animal Use and Care Committee of Nanchang University. All animal experiments were performed according to the established guidelines. The study complied with all the relevant ethical regulations on animal research.

For vivo xenograft assay: A549 cells were transfected with pCDH-Flag-GLUD1 or pCDH-Flag-GLUD1^{K503R} plasmid and constructed stable cell line overexpressing Flag-GLUD1 or Flag-GLUD1K^{503R}. A total volume of 100μl of cell suspensions (1×10^7 cells) were injected subcutaneously into the flanks of nude mice. Four weeks later, the mice were euthanized. Tumors were dissected out and their volumes and weight were measured. Tumor volume was calculated as $\pi/6 \times$ (large diameter) $\times$ (smaller diameter).[2]

Cell culture

BEAS-2B was purchased from National Collection of Authenticated Cell Clutures and cultured in RPMI 1640 (Gibco) supplemented with 10% FBS (SORFA). HEK-293T cells were cultured in MEDM (Dulbecco's Modified Eagle Media, Gibco) supplemented with 10% FBS (SORFA). Lung adenocarcinoma cell lines A549, H1299, H292, HCC827, H358, PC9, H1975 were purchased from National Collection of Authenticated Cell Clutures, SPC-A1 was purchased form BLUEFBIO and cultured in RPMI 1640 supplemented with 10% FBS (SORFA). All cells were cultured under an atmosphere of 5% CO2 at 37°C.

METHOD DETAILS

Cell growth assay

For cell proliferation assay, 3000-5000 cells in 0.5 ml RPMI 1640 with 10% FBS were seeded in 24-well plates per well, each group had three replicates. Change the medium every two days. At the 0, 2, 4, 6 days, cells were fixed with 4% formaldehyde for 15min then stained with 1% crystal violet. 10% acetic acid was used to elute the color of crystal violet and the relative proliferation was determined by the absorbance at 595 nm.

For colony formation assay, 400 cells were seeded in 6-well plates per well in 1.0 ml RPMI 1640 with 10% FBS. 10 days later, cells were fixed in 4% formaldehyde then stained with 1% crystal violet. The colonies were counted using Image J.

Reverse transcription-polymerase chain reaction (RT-PCR)

Total RNA was extracted using TRTGene reagent (Genestar P118-05). The RNA was used for reverse transcription to cDNA by Prime Script RT reagent kit with gDNA Eraser (Takara, RR047A). SYBR Green Premix Ex Taq II kit (Takara, RR820A) was perform for RT-PCR. The relative mRNA expression of target genes was

calculated using the comparative Ct method. GAPDH was used as a control for target gene. All gene primers used for RT-PCR see Table S1.

Gene overexpression and knockdown

For gene overexpression, when cells reached a density of 70–80%, the indicated plasmids were transfected into cells using the SuperFectin DNA Transfection Reagent kit (Pufei, 2102–100). 48h later, the transfection efficiencies were verified by western blot using the indicated antibodies.

For gene knockdown, when cells reached a density of 50–60%, the indicated siRNAs were transfected into cells using the siTran 2.0 siRNA transfection reagent (OriGene, TT320002). 48h later, the transfection efficiencies were verified by western blot using the indicated antibodies.

Transwell migration assay and scratch wound healing assay

For transwell migration assay, 50000 cells were seeded in 8 μm transwell chambers (Corning Costar) per well in 0.2 ml RPMI 1640 with 1% FBS. The lower chamber of the transwell device was filled with 500 μl RPMI 1640 with 10% FBS. At the indicated times, remove excess cells in the chambers using phosphate buffered saline (PBS). Cells on the lower surface of the membrane were fixed in 4% formaldehyde then stained with 1% crystal violet. Then, photographs were taken using a microscope (Olympus, IX71).

For scratch wound healing assay, cells were seeded in 6-well plates to form a confluent monolayer of 80–90% confluence in 2.0 ml RPMI 1640 with 10% FBS. Then, drawing a straight line using a 200 μl pipet tips across monolayer cell. After washing the cells three times with PBS, fresh medium with 1% FBS was added. At the indicated times, photographs were taken using a microscope (Olympus, IX71).

Immunoprecipitation and Western blot

For immunoprecipitation, cells were washed with PBS for three times. Then, cells were lysed using NP-40 buffer (20 mM Hepes, pH 7.4, 150 mM NaCl, 20 mM β-glycerol phosphates, 1 mM Na orthovanadate, 20 mM NaF, 0.5% Nonidet P-40) supplemented with protease inhibitor for 30min at 4°C. Cell lysates were centrifuged for 20 min at 4°C, then the indicated antibodies and Protein G-Agarose (Roche, 11243233001) were added to the supernatants and incubate overnight at 4°C. After that, the suspensions were centrifuged at 3000 × g for 3 min at 4°C and then washed with PBS for three times. The sediments were suspended with 2× loading buffer and boiled for 8 min.

For western blot assay, the 2× loading buffer were added to cell lysates and boiled for 8 min. The samples were subjected to 10% SDS-PAGE and then transferred to PVDF (Polyvinylidene fluoride) membranes (Millipore, IPVH00010). The PVDF membranes were blocked with 5% skim milk (Solarbio D8340) for 1 h at room temperature (25°C) and then incubated with the indicated antibodies for 12h at 4°C. The PVDF membranes washed with TBS'T for three times and then incubated with the Goat anti-Mouse/Rabbit IgG-HRP secondary antibodies for 1h at 4°C. After being washed 3 times with TBS'T, the PVDF membranes were stained with ECL detection reagent (TIANGEN, PA112-01). The images were taken using Digital gel image analysis (TANON 5500).

Measurement of GLUD1 activity

The GLUD1 activity was measured by Micro Glutamic Acid Dehydrogenase Assay Kit (Beijing Solarbio Science & Technology Co., Ltd). A549 and H1299 cells were transfected pcDNA-His-GLUD1 and pCMV-Flag-STUB1 cultured 2 days. Then, 1×10^7 cells were lysed by 1.0 ml NP-40 buffer for 30 min. The cell lysates were added Protein G-Agarose beads and anti-His antibody to incubate overnight at 4°C. The sediments were washed with PBS for 3 times and resuspended in 50 μl PBS. Then 10 μl suspension was added in 190 μl Micro Glutamic Acid Dehydrogenase Assay Kit buffer 1. 20s later, the absorbance at 340 nm was measured by Microplate Reader (A1). After 5 min 20s, the absorbance at 340 nm was measured again (A2). $\triangle$ A=(A1-A2) was used for measuring GLUD1 activity.

Stable cell lines construct

The stable cell lines were constructed using lentivirus system. The genes were synthesized by PCR with the following primers in Table S1. Then the genes were cloned into the specific vector pCDH-Flag-puro and transfected into HEK-293T cells with pSPAX2 and pMD.2G using SuperFectin DNA Transfection Reagent

kit (Pufei, 2102–100). After 48 hours, lentiviral supernatants were harvested and infected A549 cells with 5μg/mL of polybrene (SANTA CRUZ, sc-134220). Uninfected cells were killed by 4 μg/ml purinomycin (Solarbio, P8230).

Immunohistochemistry

Tumors were removed from the nude mice and fixed with 4% paraformaldehyde. Samples send to the Servicebio company for immunohistochemistry. Anti-Ki67, anti-TTF1 antibodies were purchased from Abcam (ab15580 and ab76013, #9662). Micrographs were obtained using Olympus IX71 microscope.

QUANTIFICATION AND STATISTICAL ANALYSIS

Statistical analysis was performed using GraphPad Prism 8 software. All data are presented as means ± SD. Western blot quantification was performed through Image J 1.52K software. The Student t-test was used as statistical evaluation. P-values $\leq$ 0.05 was considered statistically significant.